

Disorder in two-level atom array chirally coupled via waveguiding mode

G. Fedorovich,* D. Kornovan, and M. Petrov
ITMO University, Birzhevaya liniya 14, 199034 St.-Petersburg, Russia

In this paper we studied a one-dimensional array of quantum emitters asymmetrically coupled due to chiral interaction through a waveguiding mode. We have showed that disorder and coupling asymmetry compete with each other in forming and destroying Anderson localized states. We found that for wide range of the disorder strength there exists certain asymmetry parameter, which destroys the localization of the states. We have also numerically obtained the dependence of the critical asymmetry strength on the amplitude of the disorder. We believe that our findings are important for rapidly developing field of waveguide quantum electrodynamics, where the chiral interactions and disorder play a critical role.

Keywords: Anderson localization, chiral interaction, two-level systems, polaritonic states, waveguiding mode

I. INTRODUCTION

The coupling of quantum ensembles with nanophotonics systems such as microcavities [1], photonic crystal waveguides, [2] and optical nanofibers [3, 4] provide unique opportunities to enhance the light-matter interactions. At the same time, nanophotonic systems can also drastically modify the nature of this interactions, for example, by tailoring the polarization states of the photons and fields. This phenomenon has recently led to appearance of chiral coupling between nanophotonic modes and quantum emitters [5], i.e., coupling that depends on the propagation direction (forwards or backwards) of the light. This field has attracted even bigger interest with the emergence of topological photonics [6], where the unidirectional propagation of protected edge states became one of the central topics. Recently the quantum emitters interactions with the topological modes has been suggested as a new quantum optics platform [7–9].

In this prospective, unidirectional emitter-emitter coupling [10] and absence of back-reflection significantly modifies the character of light-matter interactions such as super- and sub-radiance [11, 12], quantum coherence [13] and disorder induced photon localization. The latter effect has vital strong importance in one-dimensional chiral quantum systems based on waveguides or topological edge states, where, on the one hand, the disorder is inevitably present due to technological imperfections, and on the other has strong impact due to low-dimensionality of the system.

The localization of excitation in disordered media stays one of the central universal concepts in modern physics [14] since its invention [15]. One-dimensional systems stand aside of others as, according to classical scaling theory [16], all the states appear to be localized. However, the situation changes drastically in non-Hermitian disordered quantum systems, where states can be either localized or delocalized [17–20]. In this sense, the chiral photonic system are strongly non-Hermitian owing to

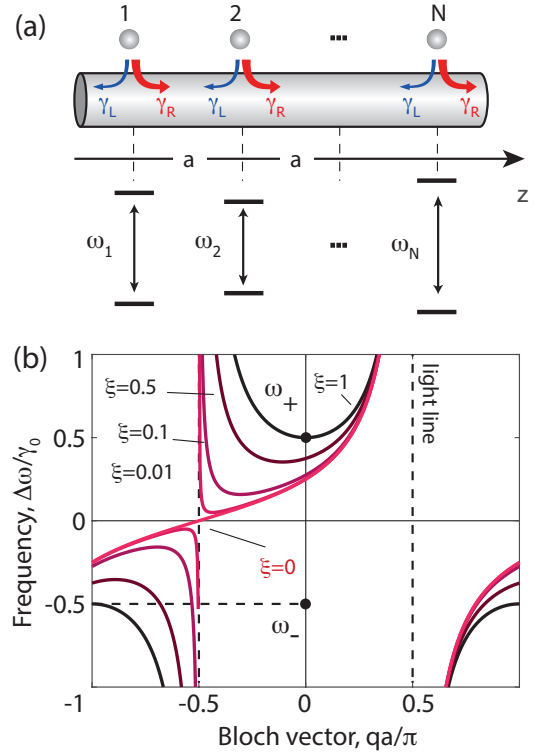


FIG. 1. a) The geometry of an array of regularly spaced quantum emitters separated with distance a and coupled through a waveguiding mode. (b) The dispersion of polaritonic modes with account for chiral interactions shown for different values of asymmetry parameter ξ .

optical losses typical for any optical system and to unidirectional character of interactions, which destroy the internal symmetry of the problem.

There have been a number of studies, which address the optical properties of chiral quantum optic systems. The interaction of guided light with disordered atomic arrays coupled to a waveguide was studied in details in Ref. [21] in the absence of chiral interactions. Alternatively, the effects of disorder on spectral properties of semiconductor polaritonic lattices have been also studied [22–24]. While light transmission through chi-

* gleb.fedorovich@metalab.ifmo.ru

ral disordered atomic arrays was considered recently in Ref. [25–27]. Namely, a complex two-parameter scaling theory of localization in chiral systems has been suggested [28]. Nevertheless, the localization properties of the eigenstates in chirally coupled quantum systems have not been discovered yet and are addressed in this paper. We believe that the results obtained in our work are important both for understanding fundamental properties of disordered quantum systems and for future development of chiral quantum optics.

The paper is organized as follows: in Sec. II we provide the general formulation of the problem; in Sec. III we focus on the optical properties of symmetric and chirally coupled arrays of two-level quantum emitters; in Sec. IV we study effects of diagonal disorder and the localization properties of the eigenstates depending on asymmetry of interaction and disorder amplitude.

II. FORMULATION OF THE PROBLEM

In our work, we consider a one-dimensional (1D) array of N two-level quantum emitters located at the coordinates z_n , and coupled through a single guided mode which is schematically shown in Fig. 1 (a).

In the case of a finite system, the effective Hamiltonian of the considered system can be represented as:

$$\hat{H} = \hat{H}_0 + \hat{V}, \quad (1)$$

$$\hat{H}_0 = \hbar \left(\omega_m - i \frac{\gamma_m}{2} \right) \sum_{m=1}^N \hat{\sigma}_m^+ \hat{\sigma}_m^-, \quad \hat{V} = \hbar \sum_{\substack{m,n=1 \\ m \neq n}}^N g_{m,n} \hat{\sigma}_n^+ \hat{\sigma}_m^-,$$

here ω_m , and γ_m are the transition frequency, and the radiative emission rate of the m -th emitter, respectively, and $g_{m,n}$ are the coupling constants. While we assume that the transition frequency may fluctuate from one emitter to another, the emission rates are fixed to be constant $\gamma_m = \gamma_0$. The coupling constants between two emitters can be defined through the electromagnetic Green's function [29, 30] $g_{m,n} = -4\pi k_0^2 \mathbf{d}_m^* \mathbf{G}(\mathbf{r}_m, \mathbf{r}_n, \omega_0) \mathbf{d}_n$, where \mathbf{d}_n is the transition dipole moment of the n -th emitter, and $k_0 = \omega_0/c$ is the wavenumber. Thus, the coupling constants are defined by the polarization properties of both the guiding mode, and the transition dipole moments, and takes the following form:

$$g_{m,n} = \begin{cases} -i \frac{\gamma_R}{2} e^{i\varphi_{mn}} & \text{for } m > n, \\ -i \frac{\gamma_L}{2} e^{i\varphi_{mn}} & \text{for } m < n, \end{cases} \quad (2)$$

where γ_R and γ_L are the photon emission rates to the right and left directions, correspondingly, and the parameter $\varphi_{mn} = k_0|z_m - z_n|$ is the phase that acquires the photon from a guided mode while travelling between the emitters at positions z_n , and z_m . Indeed, the left and right emission rates can be different: for circularly

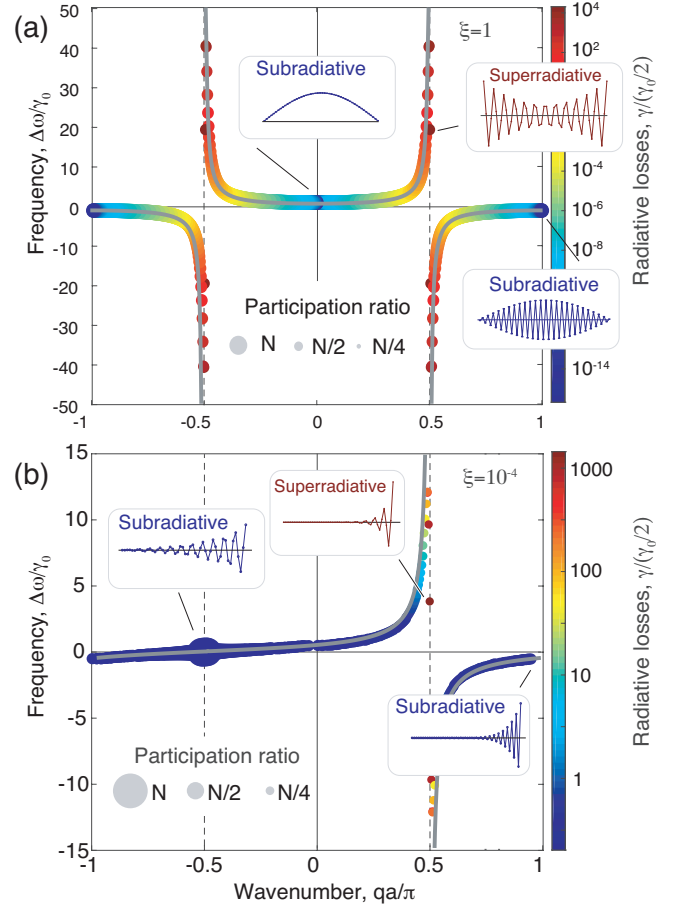


FIG. 2. (a) The resonant states of $N = 400$ symmetrically coupled ($\xi = 1$) array of quantum emitters separated with $\varphi = \pi/2$. The dispersion of the infinite system is shown with solid grey line. The color of labelling point denotes the normalized radiation loss rate for each state. The diameter of the labelling point corresponds to normalized participation ratio. The typical PR values are shown for eye guidance in the inset. The inset figures of mode profiles are plotted for $N = 50$ for clearness. (b) The resonant states of chirally coupled array with asymmetry parameter $\xi = 10^{-4}$. The computational parameters are the same as in (a).

polarized dipole transitions $\mathbf{d}_n = d_0/\sqrt{2}(\mathbf{e}_x - i\mathbf{e}_z)$ and circular polarization of the guided mode travelling in $+z$ direction $\mathbf{E}_+(z) = E_0/\sqrt{2}(\mathbf{e}_x + i\mathbf{e}_z)e^{ik_0z}$ the emission rate $\gamma_R \neq 0$, while the guided mode propagating in reverse $-z$ direction will have the opposite polarization $\mathbf{E}_-(z) = E_0/\sqrt{2}(\mathbf{e}_x - i\mathbf{e}_z)e^{-ik_0z}$, and $\gamma_L \sim |\mathbf{d}_n^* \cdot \mathbf{E}_-|^2 = 0$. Thus, one can vary the asymmetry in coupling between the emitters either by controlling the polarization of the transition dipole moment [31] or through controlling the polarization state of the guided mode [10], which provides the ground for a chiral quantum optical platform. For further convenience, we introduced the asymmetry parameter $\xi = \gamma_L/\gamma_R$, which is assumed to be freely varied from $\xi = 1$ for symmetric interaction to $\xi = 0$ for fully asymmetric interaction.

In the following sections, we will study the properties of the eigenstates of the Hamiltonian (1) describing the polaritonic modes in the ensemble of coupled emitters. We will assume that all of the emitters are ordered in an array having an equal spacing a providing a single phase parameter $\varphi_n = \varphi = k_0|z_{n+1} - z_n| = k_0a$. We will start with revising the polaritonic states in a regular array in the following section, while the system with fluctuations will be considered in Sec. IV.

III. REGULAR ARRAY OF TWO-LEVEL EMITTERS

A. Infinite periodically ordered system

First of all, it is very illustrative for further analysis to recall a photon dispersion in an infinite system of two-level quantum emitters with equal transition frequencies $\omega_n = \omega_0$ with a separation distance between the neighbors a . The interaction of emitters through the guided mode leads to the formation of polaritonic states [32–35], which dispersion $\omega(k)$ depends on the asymmetry parameter ξ and takes the form:

$$\Delta\omega(q) = -\frac{i\gamma_0}{4}(1 - \xi) + \frac{\gamma_0}{4} \left(\cot\left(\frac{\varphi - qa}{2}\right) + \xi \cot\left(\frac{\varphi + qa}{2}\right) \right), \quad (3)$$

where $\Delta\omega = \omega(q) - \omega_0$, $q \in [-\pi/a, \pi/a)$ is quasi-momentum. In the limiting cases of symmetric coupling $\xi = 1$ and ideal unidirectional coupling $\xi = 0$, the dispersion takes a simple form of

$$\Delta\omega(q) = \frac{\gamma_0}{2} \frac{\sin(\varphi)}{\cos(qa) - \cos(\varphi)}, \text{ for } \xi = 1, \\ \Delta\omega(q) = -\frac{i\gamma_0}{4} + \frac{\gamma_0}{4} \cot\left(\frac{\varphi - qa}{2}\right), \text{ for } \xi = 0. \quad (4)$$

The dispersion curve of the polaritonic states is shown in Fig. 1 (b) for a fixed period $qa = \pi/2$, and several values of the asymmetry parameter ξ . The black solid line represents the case of the symmetric coupling, clearly demonstrating the avoided crossing behaviour close to the light line. At the same time, in the case of an ideal chiral coupling, the asymmetry of the dispersion curve indicates the directional transport of the quantum excitation in the positive direction across the whole Brillouin zone. One can also notice, that the gradual change of the asymmetry parameter from $\xi = 1$ to 0 leads to closing of the band gap.

B. Finite regular chain with symmetric coupling

Once the system becomes finite, the non-zero radiative losses appear due to photon scattering at the edge of the

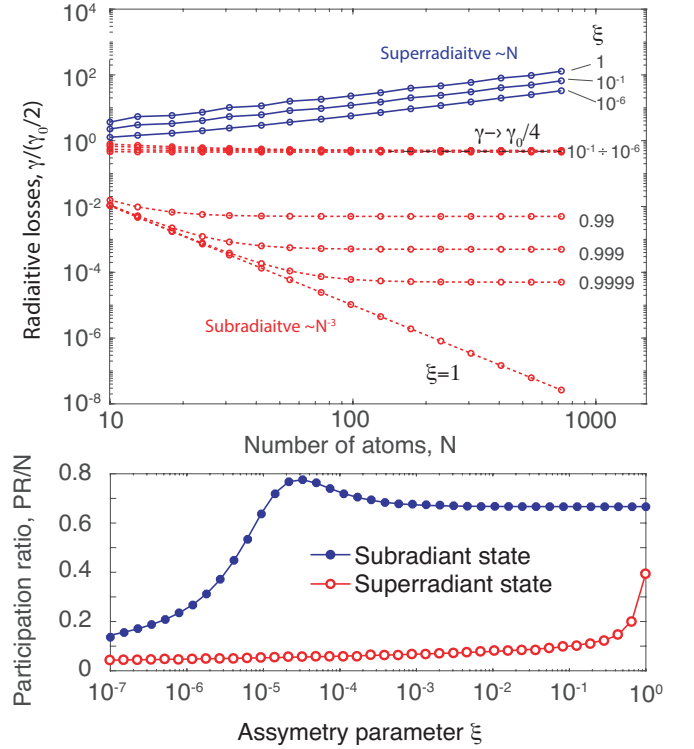


FIG. 3. (a) The radiative losses of the states with largest (superradiative) and smallest (subradiative) radiation losses as a function emitter's number for different asymmetry parameter ξ and for $\varphi = \pi/2$. (b) The participation ratio of the corresponding super- and subradiative states as a function of asymmetry parameter for $N = 400$ and $\varphi = \pi/2$.

array, and the eigenfrequencies of the collective states acquire the imaginary parts:

$$\hat{H} |\psi_k\rangle = \hbar\Omega_k |\psi_k\rangle, \quad \Omega_k = \omega_k - i\gamma_k/2.$$

In the complex plane the real and imaginary parts of eigenfrequencies from a circular structure [33] typical for Toeplitz-type matrices [36]. In order to plot the dispersion of a finite system, one can map the obtained eigenfrequencies of collective states to the first Brillouin zone of an infinite structure. The quasi-momentum q_k associated with the mode k in this case can be extracted from the corresponding modal profile $|\psi_k\rangle$, based on the modal profile [37, 38]. The eigenfrequencies for an array of $N = 100$ emitters, and phase parameter $\varphi = \pi/2$ are plotted in Fig. 2 for (a) symmetric, and (b) asymmetric coupling. They form a discrete set of points on the dispersion line of the infinite system (grey solid line in Fig. 2). The color of points in the figure denote the radiative decay rates for each particular state, clearly showing that the states close to the band edge have the smallest decay rate (subradiant), while the states close to the anticrossing region possess the strongest radiative losses due to the coupling with the waveguiding mode. In the insets, we plot the distribution of wavefunction amplitudes in the following representation: $|\psi_k\rangle = \sum_n c_{nk} |n\rangle$ for sub-

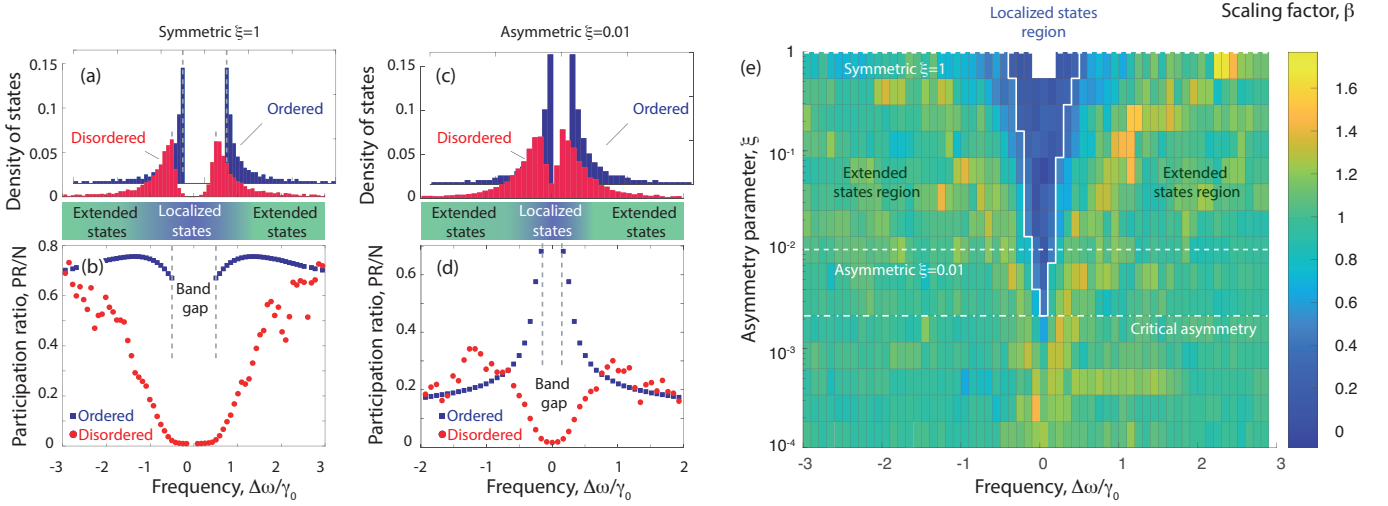


FIG. 4. (a) Density of states of the ordered ($\delta = 0$) and disordered ($\delta = 0.01$) symmetric system. (c) The dependence of PR for the systems shown in (a): blue squares correspond to ordered system, and red circles to disordered. (b) Density of states of the ordered ($\delta = 0$) and disordered ($\delta = 0.01$) chiral system ($\xi = 0.01$). (d) The dependence of PR for the systems shown in (c): blue squares correspond to ordered system, and red circles to disordered. (e) The spectral map of the scaling factor β as function of frequency detuning $\Delta\omega$ and asymmetry parameter ξ for fixed disorder amplitude $\delta = 0.01$. The blue region corresponds to localized states, while the green one to delocalized. The dashed lines denote $\xi = 1$ and $\xi = 0.01$ region corresponding to the cases plotted in (a)-(d). The critical asymmetry dash-dot line denote the critical value of ξ after which all the states become delocalized. The simulations parameter for (a)-(e) are $N = 400$ and $\varphi = \pi/2$. The number of random realizations for averaging was equal to 1000 for (a)-(d), and 500 for (e).

radiant, and superradiant states, where $|n\rangle$ state corresponds to n -th emitter being excited, while all the others are in the ground state: $|n\rangle = |e_n\rangle|g\rangle^{\otimes(N-1)}$. The mode structure of these states has an envelope and a Bloch-type phase factor and partially inherits their structure from the nearest neighbour model [37, 39]. The radiative losses of subradiant and superradiant states scale with the size of the system as $\gamma_{sub} \propto N^{-3}$ [39, 40], while the emission rates of superradiant states $\gamma_{sup} \propto N$ [21, 41]. This can be clearly seen from Fig. 3 (a), where the radiative losses of superradiant and subradiant states are plotted in double logarithmic scale as functions of the emitter number N for various values of the asymmetry parameter ξ .

Finally, the last parameter, which characterizes the eigenstates, and has a critical importance for identification of localization effects is the participation ratio (PR) [42], that quantifies the effective number of the occupied sites by a single excitation, and which can be expressed as:

$$PR_k = \frac{\sum_{i=1}^N |c_{ik}|^2}{\sum_{i=1}^N |c_{ik}|^4}, \quad (5)$$

for the k -th state. Since in the case of the ordered structure, the eigenmodes of the system are constructed from the Bloch waves, the excitation occupies almost all of the lattice sites $PR \sim N$. We have depicted the normalized participation ratio PR/N for each mode in Fig. 2 (a)

with the diameter of the circle labelling the PR value for each state. One can see, that the superradiative states have the smallest PR , while the subradiant states, on the contrary, are the most distributed but still having $PR \approx N$. Moreover, all the states in the ordered array scale linearly with the system size, so $PR \propto N$, which is a sign of their truly extended nature.

One also needs to mention a special case of $\varphi = 0$, which corresponds to discrete Bardin-Cooper-Schiffer model [43, 44] and is proposed for description of superconducting states in lattice models. In this case, there appear $N - 1$ degenerate states with zero radiative rate and one non-degenerate state, which has superradiative character with $\gamma_N = N\gamma_0$ and constant mode profile with in-phase amplitudes $|\psi\rangle = 1/\sqrt{N} \sum_n |n\rangle$.

C. Finite regular chain with asymmetric coupling

Once the chiral coupling is introduced for a finite system, discrete resonant states follow the dispersion behavior of the infinite structure as shown with a solid grey line in Fig. 2 (b). One can see that the anticrossing at $qa = \varphi$ vanishes in the negative region of the Brillouin zone, and the resonant states close to this point possess the lowest radiative losses among all of the states that are comparable to γ_0 in value. Thus, the absence of backscattering in an array of asymmetrically coupled emitters destroys the subradiance effect, which bases on the destructive interference of radiation coming from emitters. At the

same time, the radiative losses of superradiant state in the case of chiral coupling stay of the same order as in the system with the symmetric coupling. These effects can be clearly seen from Fig. 3 (a), where radiative losses of subradiant, and superradiant states are shown for a wide range of ξ parameter. While losses of subradiant states become constant with the increasing emitter number N , and behave like $\gamma_{sub} \rightarrow \gamma_0/4(1-\xi)$ (see Eq. (3)) for large N [12], the superradiant state losses tend to $\gamma_{sup} \rightarrow N\gamma_0$ for $\xi \rightarrow 0$, and large N .

Subradiant states have the largest PR value close to N , therefore, the excitation occupies most of the array sites as shown by the label diameter Fig. 2 (b). However, now the modes become localized at the edge of the chain as it is shown in the insets of Fig. 2 (b). If ξ becomes small enough the excitation in the system noticeably prevails on the right side of the chain. This is explained by the fact that each emitter radiates to the left side much weaker than to the right in the asymmetric coupling case. In the limit $\xi \rightarrow 0$ almost all eigenstates become degenerate, and only one non-trivial state survives $|\psi\rangle = |N\rangle$. The participation ratio strongly depends on the asymmetry parameter, which is reflected in Fig. 3 (b), where the value of PR is plotted for the states with the highest and lowest radiative losses. One can see that as $\xi \rightarrow 0$ the PR decreases reaching value of $PR \approx 1$ for the limiting case. But the important fact is that despite PR for chirally coupled emitters becomes much smaller than N , our calculations show that the states are still extended as scaling behaviour $PR(N, \xi \rightarrow 0) \propto N$ is observed.

IV. DISORDER IN THE ARRAY

Finally, in this section we will focus on the effects of localization induced by diagonal disorder due to the fluctuations of transition frequencies of k -th emitter: $\omega_k = \omega_0 + \Delta\omega_k$, where $\Delta\omega_k$ is normally distributed random value with standard deviation equal to $\delta \cdot \gamma_0$ in the absence of correlations between the emitters.

A. Disorder in an array with achiral coupling

The effects of disorder in long-range interacting systems have been studied in a number of previous works with focus on cold atoms coupled to through a waveguiding mode [21], and exciton-polaritons in one-dimensional photonic crystal structures [23, 34]. Most of them were addressing the effects of Anderson localization due to diagonal [22], and positional (off-diagonal) [21, 23] disorder, and related spectral properties of the system such as inhomogeneous broadening of reflection or transmission coefficients. In this section, will overview the effects of diagonal disorder on the localization properties of the system eigenmodes.

We start with the density-of-states (DOS) function as a proper measure of disordered structures. The DOS

profiles shown in Fig. 4 (a) have typical structure that can be understood from the dispersion curves shown in Fig. 1: they have a band gap width equal to γ_0 in case of $\varphi = \pi/2$, and possess van Hove singularities typical for one-dimensional systems. One can notice, that introduction of disorder leads to the smearing of the band edges, and formation of the Urbach tails [42]. The normalized value of PR drastically drops in the are close to the band gap as shown in Fig. 4 (b). At the the same time, the states far from the band gap edge are spread over the large number of sites that is close to N .

The large relative value of PR does not immediately provides the delocalization of the eigenstates. In order to check that, we have traced the exponent parameter β in the scaling behaviour of the $PR(N) \propto N^\beta$. The spectral dependence of the scaling factor $\beta(\Delta\omega)$ is shown in Fig. 4 (e) for different values of the asymmetry parameter ξ . One can see that for the symmetric case $\xi = 1$ the states close to the band edge appear to be localized as β is close to 0 providing that the localization length does not scale up with the system size. Meanwhile, far from the band gap region the states are clearly delocalized, despite the 1D nature of the system. The absence of localization for most of the states is provided by a non-Hermitian character of the problem [17]. Note that Haakh et al. [21] have related the delocalization of states to a quasi-3D nature of the interaction as in their report the vacuum dipole-dipole interaction was also considered, and the coupling efficiency to the guided mode was less than 1. Clearly, that is not the case for the system considered in this work as there is no free space coupling, and yet not all of the states are localized.

With the decrease of the asymmetry parameter ξ the band gap gets narrower as can be seen in DOS spectra in Fig. 4 (c) for $\xi = 0.01$, and the localization region also becomes narrower (see Fig. 4 (d)). The spectral width of the localized states region reduces with the further decrease of the asymmetry parameter, and once the asymmetry parameter reaches the critical value all states become delocalized (see Fig. 4 (e) below the dash-dot line). This occurs once the band gap width becomes comparable to the energy smearing due to disorder, when, roughly speaking, Urbach tails are greater or equal to the band gap size. We believe that the map shown in Fig. 4 (e) is one of the most important results of the paper, clearly demonstrating the delocalization transition driven by chiral interactions in the disordered system.

In order to illustrate the competing effects of disorder and asymmetry on Anderson localization, we have analyzed the delocalization transition for different values of the disorder amplitude δ , while the results shown in Fig. 4 were obtained for a fixed value of disorder amplitude δ . Fig. 5 (a) shows the dependence of the normalized PR on the disorder amplitude δ , and asymmetry parameter ξ for states in a band gap close to its edge as shown in Fig. 4 (e). One can see that for symmetric case, and for small disorder the states extend over the whole length of the system. With the increase of disorder amplitude δ

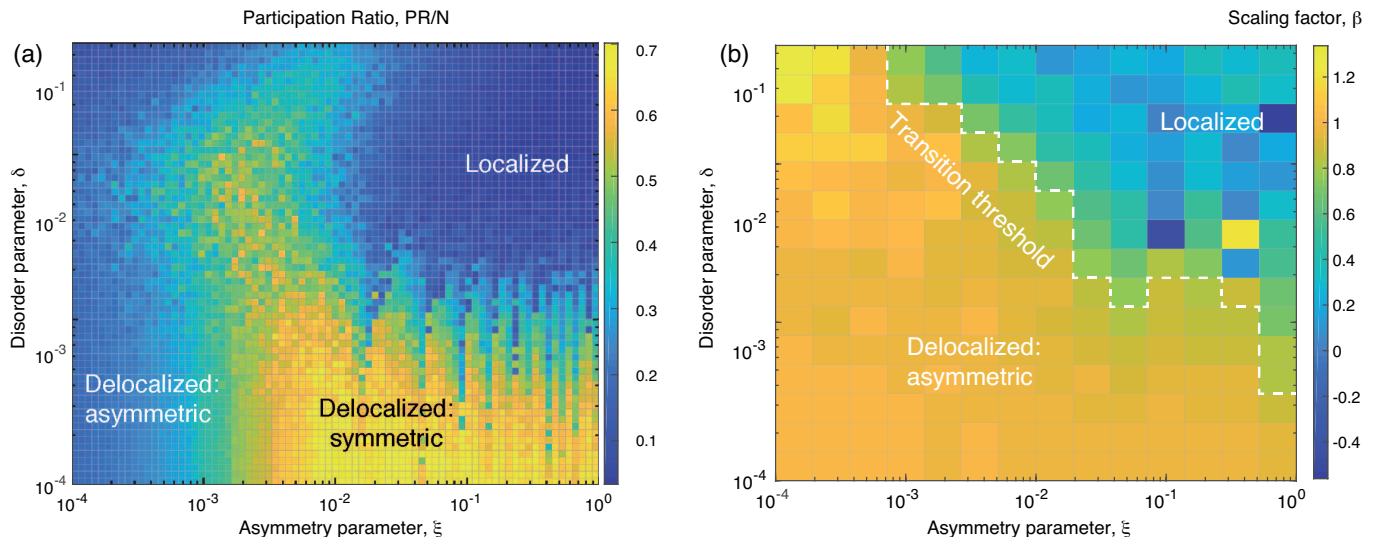


FIG. 5. (a) Dependence of the PR of the state close to band-edge on the asymmetry parameter ξ and disorder amplitude δ for array of $N = 100$ emitter, averaged over 500 realizations. (b) The spectral map of the scaling factor β as function of asymmetry parameter ξ and disorder amplitude δ . The blue region corresponds to localized states, while the yellow one to delocalized. The calculations were provided for an array of $N = 400$ emitters with averaging over 100 realizations.

the states become localized and $PR/N \lesssim 0.1$, which is as a sign of localization. However, at small enough asymmetry parameter $\xi \sim 10^{-3}$ the state occupies a small fraction of the system comparable to localized state, but that is due to chiral coupling rather than disorder. As discussed in Sec. III, in case of strong chiral coupling the excitation is located at the right edge of the system, and its normalized PR tends to 0 as $\xi \rightarrow 0$. Despite of that, it stays delocalized in the sense of scaling of the PR parameter with the system size N . To prove that, we have plotted a map of a scaling factor β shown in Fig. 5 (b) in parallel to PR map in (a). One can see, that $\beta \sim 0$ for the upper right region where the disorder is strong enough to form localized state, and chirality is weak enough not to destroy it. At the same time, to the left of the delocalization transition line the β -factor is close to $\beta \sim 1$, which is a clear sign of a delocalized character of the state. We have marked the transition region separating the localized and of delocalized areas with a dashed line for eye guidance.

V. CONCLUSION

Concluding, we have considered a one-dimensional array of two-level emitters coupled through a waveguiding

modes with account for chiral interaction. Introduction of the disorder in such system results in partial localization of the eigenstates, which can be destroyed by chiral nature of the interaction. We show that for particular strength of the interaction asymmetry all the states become delocalized, forced by the unidirectional propagation of excitation in chiral system. There exists certain competition between the disorder and coupling asymmetry strengths and the critical values of the asymmetry strength have been identified numerically.

We believe that our findings will be important for rapidly developing field of waveguide-QED, where the chiral interactions and disorder play a critical role. Moreover, extension of the obtained results to multiphoton domain will be of significant interest due to rapid development of theoretical[45–47] and experimental studies in this area[13, 48].

VI. ACKNOWLEDGEMENT

The authors are thankful to Diedrik Wiersma, Ivan Iorsh, and Vladimir Yudson for fruitful discussions.

[1] M. Scheucher, A. Hilico, E. Will, J. Volz, and A. Rauschenbeutel, *Science* **354**, 1577 (2016), arXiv:1609.02492.

[2] J. D. Hood, A. Goban, A. Asenjo-Garcia, M. Lu, S. P. Yu, D. E. Chang, and H. J. Kimble, *Proceedings of the National Academy of Sciences of the United States of America*, arXiv:1603.02771.

- [3] E. Vetsch, D. Reitz, G. Sague, R. Schmidt, S. T. Dawkins, and A. Rauschenbeutel, *Physical Review Letters* **104**, 203603 (2010).
- [4] S. T. Dawkins, R. Mitsch, D. Reitz, E. Vetsch, and A. Rauschenbeutel, *Physical Review Letters* **107**, 243601 (2011).
- [5] P. Lodahl, S. Mahmoodian, S. Stobbe, A. Rauschenbeutel, P. Schneeweiss, J. Volz, H. Pichler, and P. Zoller, *Nature* **541**, 473 (2017).
- [6] L. Lu, J. D. Joannopoulos, and M. Soljačić, *Nature Photonics* **8**, 821 (2014), arXiv:1408.6730.
- [7] S. Barik, A. Karasahin, S. Mittal, E. Waks, and M. Hafezi, *Physical Review B* **101**, 1 (2020), arXiv:1906.11263.
- [8] M. Jalali Mehrabad, A. P. Foster, R. Dost, A. M. Fox, M. S. Skolnick, and L. R. Wilson, *arXiv* **7** (2019), 10.1364/optica.393035, arXiv:1912.09943.
- [9] M. Jalali Mehrabad, A. P. Foster, R. Dost, E. Clarke, P. K. Patil, I. Farrer, J. Hefernan, M. S. Skolnick, and L. R. Wilson, *Applied Physics Letters* **116** (2020), 10.1063/1.5131846, arXiv:1910.07448.
- [10] A. Aiello, P. Banzer, M. Neugebauer, and G. Leuchs, *Nature Photonics* **9**, 789 (2015).
- [11] F. Le Kien and A. Rauschenbeutel, *Physical Review A* **95**, 1 (2017), arXiv:arXiv:1612.04516v1.
- [12] D. Kornovan, M. Petrov, and I. Iorsh, *Physical Review B* **96**, 115162 (2017), arXiv:1701.06311.
- [13] A. S. Prasad, J. Hinney, S. Mahmoodian, K. Hammerer, S. Rind, P. Schneeweiss, A. S. Sørensen, J. Volz, and A. Rauschenbeutel, *Nature Photonics* **14**, 719 (2020), arXiv:1911.09701.
- [14] A. Lagendijk, B. Van Tiggelen, and D. S. Wiersma, *Physics Today* **62**, 24 (2009).
- [15] P. W. Anderson, *Physical Review* **109**, 1492 (1958).
- [16] E. Abrahams, P. W. Anderson, D. C. Licciardello, and T. V. Ramakrishnan, *Physical Review Letters* (1979), 10.1103/PhysRevLett.42.673.
- [17] N. Hatano and D. R. Nelson, *Physical Review Letters* **77**, 570 (1996).
- [18] P. Brouwer, P. Silvestrov, and C. Beenakker, *Physical Review B - Condensed Matter and Materials Physics* **56**, R4383 (1997).
- [19] P. W. Brouwer, C. Mudry, B. D. Simons, and A. Altland, *Physical Review Letters* **81**, 862 (1998).
- [20] F. Hébert, M. Schram, R. T. Scalettar, W. B. Chen, and Z. Bai, *European Physical Journal B* **79**, 465 (2011).
- [21] H. R. Haakh, S. Faez, and V. Sandoghdar, *Physical Review A* **94**, 1 (2016).
- [22] G. Malpuech and A. Kavokin, *Semiconductor Science and Technology* **14**, 1031 (1999).
- [23] V. A. Kosobukin, *Physics of the Solid State* **45**, 1145 (2003).
- [24] V. A. Kosobukin and A. N. Poddubnyĭ, *Physics of the Solid State* **49**, 1977 (2007).
- [25] I. M. Mirza, J. G. Hoskins, and J. C. Schotland, *Physical Review A* **96**, 30 (2017), arXiv:1708.00902.
- [26] I. M. Mirza and J. C. Schotland, *Journal of the Optical Society of America B* **35**, 1149 (2018), arXiv:1709.04641.
- [27] H. H. Jen, *Physical Review A* **102**, 1 (2020), arXiv:2005.09855.
- [28] K. Kawabata and S. Ryu, , 1 (2020), arXiv:2005.00604.
- [29] T. Gruner and D.-G. Welsch, *Physical Review A* **53**, 1818 (1996).
- [30] A. Asenjo-Garcia, J. D. Hood, D. E. Chang, and H. J. Kimble, *Physical Review A* **95**, 1 (2017).
- [31] R. J. Coles, D. M. Price, J. E. Dixon, B. Royall, E. Clarke, P. Kok, M. S. Skolnick, A. M. Fox, and M. N. Makhonin, *Nature Communications* **7**, 1 (2016).
- [32] E. Ivchenko, A. Nesvizhskii, and S. Jorda, *Superlattices and Microstructures* **36**, 1156 (1994).
- [33] M. R. Vladimirova, E. L. Ivchenko, and A. V. Kavokin, *Semiconductors* **32**, 90 (1998).
- [34] G. Angelatos and S. Hughes, *Optica* **3**, 370 (2016), arXiv:arXiv:1509.01613v1.
- [35] D. F. Kornovan, A. S. Sheremet, and M. I. Petrov, *Physical Review B* **94**, 245416 (2016), arXiv:arXiv:1608.03202v1.
- [36] R. Movassagh and L. P. Kadanoff, *Journal of Statistical Physics*, Vol. 167 (Springer US, 2017) pp. 959–996, arXiv:1604.08295.
- [37] W. H. Weber and G. W. Ford, *Physical Review B* **70**, 125429 (2004).
- [38] M. Petrov, *Physical Review A* **91**, 023821 (2015).
- [39] A. Asenjo-Garcia, M. Moreno-Cardoner, A. Albrecht, H. J. Kimble, and D. E. Chang, *Physical Review X* **7**, 1 (2017), arXiv:1703.03382.
- [40] Y.-X. Zhang, C. Yu, and K. Mølmer, *Physical Review Research* **2**, 1 (2020).
- [41] R. H. Dicke, *Physical Review* **93**, 99 (1954).
- [42] B. Van Tiggelen, *Localization of waves* (1999).
- [43] R. Modak, S. Mukerjee, E. A. Yuzbashyan, and B. S. Shastry, *New Journal of Physics* **18** (2016), 10.1088/1367-2630/18/3/033010, arXiv:1503.07019.
- [44] G. L. Celardo, R. Kaiser, and F. Borgonovi, *Physical Review B* **94**, 1 (2016), arXiv:1604.07868.
- [45] A. N. Poddubny, *arXiv* **1908.01818** (2019), arXiv:1908.01818.
- [46] S. Mahmoodian, M. Čepulkovskis, S. Das, P. R4383 (1997). K. Hammerer, and A. S. Sørensen, *Physical Review Letters* **121**, 1 (2018), arXiv:1803.02428.
- [47] S. Mahmoodian, G. Calajó, D. E. Chang, K. Hammerer, and A. S. Sørensen, *arXiv* **1910.05828** (2019), arXiv:1910.05828.
- [48] I. S. Besedin, M. A. Gorlach, N. N. Abramov, I. Tsitsilin, I. N. Moskalenko, A. A. Dobronosova, D. O. Moskalev, A. R. Matanin, N. S. Smirnov, I. A. Rodionov, A. N. Poddubny, and A. V. Ustinov, *arXiv* (2020), arXiv:2006.12794.